Available online at www.sciencedirect.com
ScienceDirect
Bioorganic & Medicinal Chemistry 15 (2007) 3635–3648
Bioorganic & Medicinal Chemistry

Dual irreversible kinase inhibitors: Quinazoline-based inhibitors incorporating two independent reactive centers with each targeting different cysteine residues in the kinase domains of EGFR and VEGFR-2

Allan Wissner,* Heidi L. Fraser, Charles L. Ingalls, Russell G. Dushin, M. Brawner Floyd, Kinwang Cheung, Thomas Nittoli, Malini R. Ravi, Xingzhi Tan and Frank Loganzo

Chemical and Screening Sciences and Oncology Research, Wyeth Research, 401 N. Middletown Road, Pearl River, NY 10965, USA

Received 8 November 2006; revised 14 March 2007; accepted 18 March 2007
Available online 23 March 2007

Abstract—A series of 4-dimethylamino-but-2-enoic acid [4-(3,6-dioxo-cyclohexa-1,4-dienylamino)-7-ethoxy-quinazolin-6-yl]-amide derivatives were prepared. These compounds have two independent reactive centers and were designed to function as dual irreversible inhibitors of the kinase domains of both Epidermal Growth Factor Receptor (EGFR) and Vascular Endothelial Growth Factor Receptor-2 (VEGFR-2) where each reactive center targets a different, non-conserved, cysteine residue located in the ATP binding pocket of these enzymes. The compounds contain a 6-(4-(dimethylamino) crotonamide) Michael acceptor group that targets Cys-773 in EGFR and a 4-(amino-[1,4]benzoquinone) moiety that targets Cys-1045 in VEGFR-2. In vitro studies indicated that most of these compounds are relatively potent inhibitors of each enzyme. These inhibitors were compared with reference compounds that lack one or both of the reactive centers. The relative dependence of the IC_{50} values on the concentration of ATP used in the assays suggests that these compounds appear to function as irreversible inhibitors of each kinase.

1. Introduction

There has been a considerable effort to design small-molecule irreversible inhibitors of kinase targets for the treatment of cancer.[1,2] Compared to conventional ATP-competitive inhibitors, irreversible kinase inhibitors have a number of both potential and realized advantages. It is frequently observed that irreversible kinase inhibitors show enhanced potency when compared to structurally similar conventional inhibitors. There is also the expectation that an irreversible inhibitor need not exhibit prolonged circulating blood levels to achieve a desired biological effect. Once the target enzyme is deactivated by covalent bond formation, the biological effect should persist even after the drug leaves the circulation. In effect, the duration of action of such a drug will be a function of the rate of enzyme turnover.

Furthermore, it has recently been observed that certain irreversible inhibitors can inhibit the function of kinases that have mutated and developed resistance to conventional inhibitors. For example, Kwak and coworkers[3] have shown that the compounds **1** (EKB-569) and **2** (HKI-272), both 4-anilinoquinoline-3-carbonitrile-based irreversible inhibitors, designed to covalently bind to a conserved cysteine residue present in some erbB kinase family members, retained activity against Erlotinib- and Gefitinib-resistant cell lines. Moreover, in contrast to the conventional reversible inhibitors, it proved extremely difficult to induce resistance in cells with **1** and **2**. Similar results were obtained in a related study by Cater et al. for the irreversible EGFR kinase inhibitors **1** and **3** (CI-1033).[4] Additionally, it was observed that the quinazoline-based irreversible EGFR kinase inhibitor **4** (EKI-785) retained inhibitory activity against resistant cell lines.[5–7] In a clinical study, some patients with non-small cell lung cancer having an acquired resistance to Gefitinib responded to treatment with **1**.[8]

Keywords: Dual; Irreversible; Kinase; Inhibitors; Quinazoline-based; Independent reactive centers; Cysteine residues; EGFR; VEGFR-2; KDR; Quinone; Michael acceptor; Epidermal; Growth; Factor; Receptor; Vascular; Endothelial.
* Corresponding author. Tel.: +1 845 602 3580; fax: +1 845 602 5561; e-mail: wissnea@wyeth.com

0968-0896/$ - see front matter © 2007 Elsevier Ltd. All rights reserved.
doi:10.1016/j.bmc.2007.03.055

When appropriately designed, irreversible inhibitors can show enhanced selectivity. Cohen et al. have shown that covalent binding inhibitors based on a pyrrolo[2,3-*d*]pyrimidine scaffold showed remarkable specificity toward kinases of the RSK family.[9] It was postulated that the selectivity exhibited by these compounds was a result of covalent binding to a conserved cysteine residue present in members of the family combined with functionality on the inhibitors intended to interact within the gatekeeper region of the protein. Finally, it has been suggested that irreversibly binding EGFR inhibitors might make useful molecular imaging agents for cancer.[10,11]

Contrasting with the potential advantages of these covalent binding kinase inhibitors is a possible liability that they might indiscriminately react with non-target related proteins. This could be manifested as an increased toxicity. Therefore, it is important, if these covalent binding agents are to make useful drugs, that they should not have excessive reactivity and that they should be appropriately constructed to have a reasonably good fit at the active site of the target with the reactive centers oriented in the proper manner for a covalent interaction to ensue. Such a drug, for example, one that is designed to react with an active site cysteine residue, needs to be more reactive toward the target enzyme than it is toward other nucleophilic species (such as glutathione (GSH), or other proteins), which may be present in high concentrations in the circulation or in the cytosol. In designing an irreversible inhibitor, one can rely on an anticipated entropic effect wherein the rate of reaction of such an inhibitor, when bound at the active site with the correct orientation, will be enhanced relative to the rate of reaction when in solution, due to the fact that the reactive centers on both the protein and drug will be held in close proximity. Under these circumstances, the local concentration of the reacting partners will be much higher when the drug is bound to its target compared to when the components are free in solution. This phenomenon has been measured with the irreversible kinase inhibitor hypothemycin.[12]

In an earlier project, we successfully produced covalent binding inhibitors of EGFR and Her2 kinases.[13–17] These inhibitors had either a quinazoline or quinoline-3-carbonitrile core structure. Two members of the latter series, **1** and **2**, have entered clinical trials. Other workers have arrived at some similar compounds.[18] These inhibitors are able to covalently interact with the target proteins by virtue of the fact that they undergo a Michael addition reaction with a conserved, solvent exposed, cysteine residue present in these enzymes (Cys-773 in EGFR and Cys-805 in Her2). We showed that the 4-(dimethylamino)crotonamide Michael acceptor group present on these inhibitors is a particularly effective one for this purpose. We demonstrated that the terminal dimethylamino group of this Michael acceptor serves as an intramolecular catalyst for Michael addition reactions in solution and we have proposed that it has a similar role when the inhibitor is bound at the active site of these enzymes. More recently, we described our work on a series of irreversible inhibitors of VEGFR-2 as exemplified by the quinazoline derivative **5**.[19] For these compounds, we proposed that covalent bond formation with the enzyme is the result of a initial redox reaction between the quinone ring of the inhibitor and Cys-1045 located within the ATP binding pocket of the enzyme, resulting in the formation of a semiquinone species and a sulfhydryl radical. The combination of these radicals resulted in a reductive addition of the cysteine sulfhydryl group to the quinone ring. Here, we note that the targeted cysteine in EGFR is not conserved in VEGFR-2 and that the VEGFR-2 targeted cysteine is not conserved in EGFR. Since both EGFR and VEGFR-2 inhibitors having a quinazoline core structure were used in the past for the construction of both conventional ATP-competitive inhibitors as well as irreversible inhibitors, we hypothesized that it might be possible to design molecules, using this scaffold, that have two different reactive centers, one designed to form a covalent interaction with the Cys-773 in EGFR and the other designed to form a covalent interaction with the Cys-1045 in VEGFR-2. An inhibitor of this type would then function as an irreversible inhibitor of each enzyme, but one that targets a different cysteine in each case. In this work, we will describe the preparation of some quinazoline derivatives such as **6** that combined the Michael acceptor functionality of our earlier series of EGFR inhibitors with the quinone ring of our VEGFR-2 inhibitors and we will present our evidence from in vitro enzyme studies showing that these compounds appear to function as we propose. To our knowledge, the preparation of a molecule that has two separate reactive groups, each designed to target, via a covalent interaction, a different cysteine residue in unrelated enzymes, is unprecedented in the literature.

Moreover, one could imagine that combining EGFR and VEGFR-2 kinase inhibitory activities in a single molecule could result in a useful entity having anti-cancer applications. In the former case, the inhibitor will be targeting a growth factor receptor that is deregulated, either by overexpression or mutation, in a number of malignancies[20–23] while in the latter case, the inhibitor will be targeting a growth factor receptor which the tumor depends upon to build and maintain its vasculature.[24–27]

2. Chemistry

The compounds were prepared as shown in Scheme 2. Nitration of **7**,[28] as previously described,[29] gave a mixture of isomers from which pure **8** could be obtained after recrystallization from acetic acid. Replacement of the fluorine with an ethoxy group was accomplished by heating with sodium ethoxide in ethanol at reflux. The resulting intermediate **9** was chlorinated by heating in thionyl chloride at reflux in the presence of a catalytic quantity of DMF. Displacement of the 4-chloro group of **10** with 4-chloro-2,5-dimethoxyaniline was accomplished by heating in isopropanol at reflux. Reduction of the nitro group of **11** using iron and acetic acid in methanol gave intermediate **12**. The 4-(dimethylamino)crotonamide Michael acceptor group was

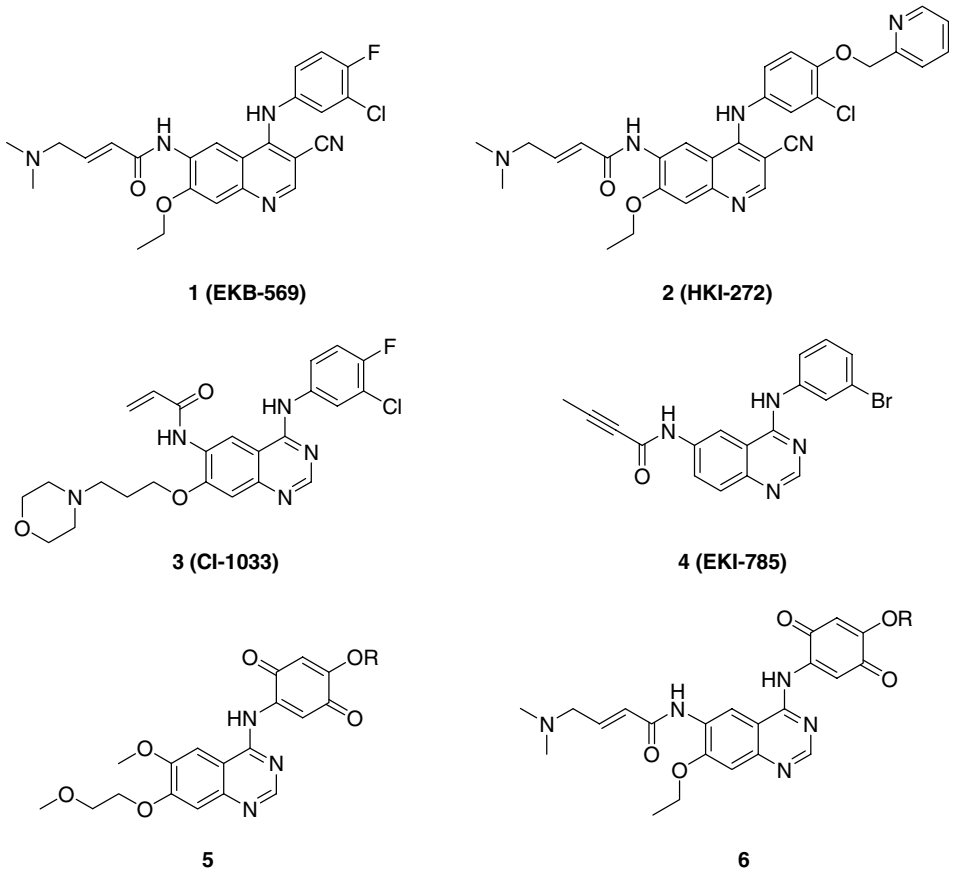

Scheme 1.

incorporated by the reaction of **12** with the acid chloride derived from (*E*)-4-(dimethylamino)crotonic acid. Oxidation of **13** to the quinone derivative **14** was achieved using ceric ammonium nitrate (CAN) in aqueous acetonitrile at room temperature. We found that **14** is a highly reactive species and is relatively unstable in the absence of solvent. Therefore, we found it best to isolate **14** in a chloroform or methylene chloride solution and to use it in that manner without additional purification. The reaction of **14** with various alcohols, in the presence of triethylamine or sodium phenoxide as catalysts, then furnished inhibitors **15**–**24** in modest yields.

In our earlier study of the irreversible VEGFR-2 inhibitors,[19] we surveyed a large variety of substituents attached to the quinone ring. We showed that the reactivity of the resulting molecules correlated with their LUMO energy and that there was a tendency for the potency of the inhibitors to be related to their reactivity. In this study, we decided to incorporate substituents on the quinone ring having a narrow spectrum of reactivity based on the earlier calculations of the LUMO energies and kinetic studies for related compounds. One group of compounds that were generally potent inhibitors, but which had relatively moderate reactivity, were those with 4-benzyloxy groups on the quinone ring. Furthermore, in our EGFR and Her2 projects,[17] we observed that compounds with 4-(4-benzyloxy-phenylamino) groups were usually potent inhibitors of those enzymes. Therefore, in the present study, many of the quinone substituents we incorporated are of that type. Additionally, as will be shown by our molecular modeling results, such inhibitors set up a favorable interaction between the phenyl ring of the benzyloxy group and a phenylalanine residue that is present in both EGFR and VEGFR-2. This likely results in better initial binding affinity and helps position the quinone ring toward Cys-1045 of VEGFR-2 with the proper orientation to initiate a redox reaction.

In addition to preparing these dual irreversible inhibitors, we needed to have available some reference compounds with which to compare their inhibitory properties. Compound **27** was prepared as shown in Scheme 3. This compound was prepared assuming, based on its structure, it would function as an irreversible EGFR inhibitor and a reversible VEGFR-2 inhibitor. The compound incorporates the Michael acceptor functional group of our earlier EGFR inhibitors but it also has a 4-substituent on the quinazoline core that is known to confer ATP-competitive VEGFR-2 inhibitory activity on this class of compounds.[30,31] Accordingly, the quinazoline derivative **25**[32] was acylated with the acid chloride derived from (*E*)-4-(dimethylamino)crotonic acid. Heating a mixture of **26** and 4-bromo-2-fluoro aniline in a mixture of NMP and isopropanol in the presence of a catalytic amount of pyridine hydrochloride furnished **27**.

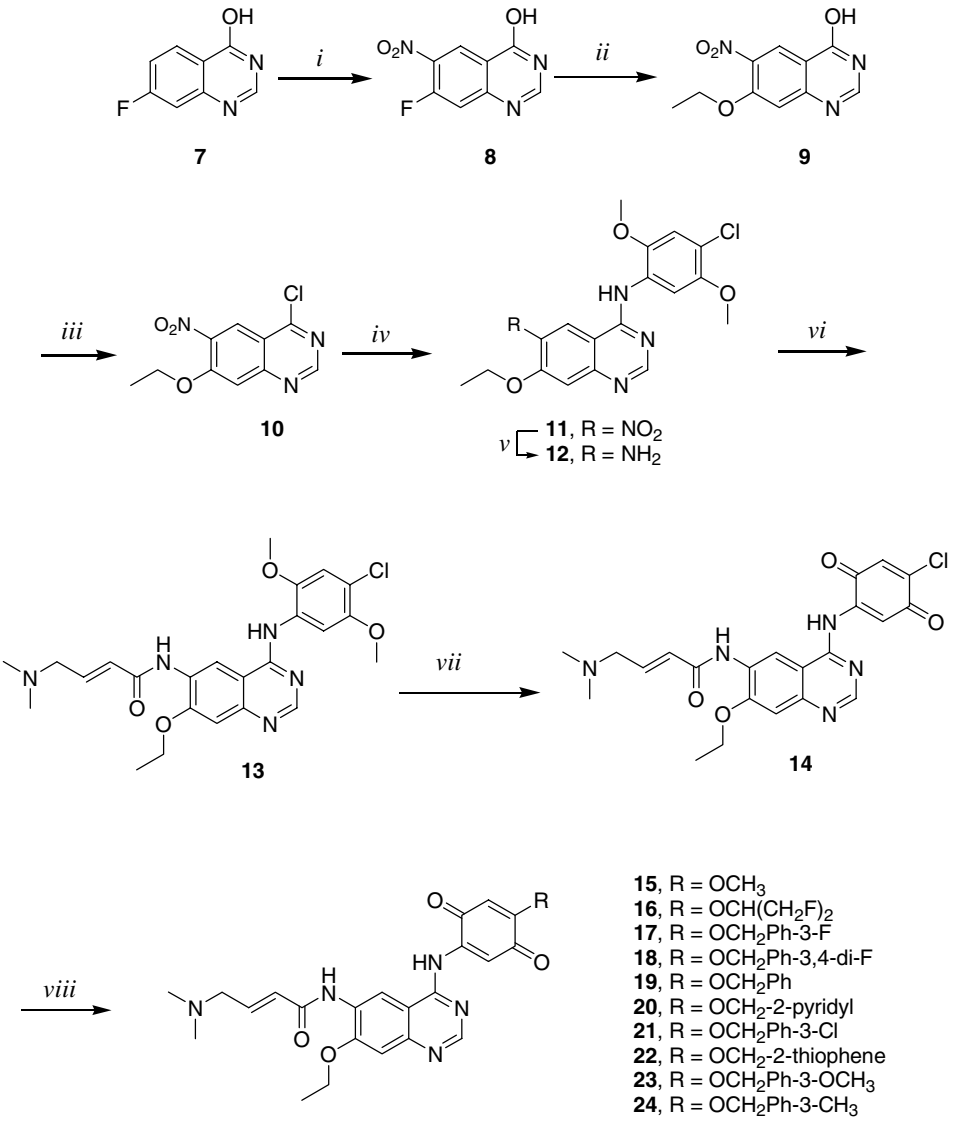

Scheme 2. Reagents and conditions: (i) H_2SO_4, HNO_3, 100 °C, 1 h; (ii) NaOEt, EtOH, reflux, 1.5 h; (iii) $SOCl_2$, DMF (cat), reflux, 3.5 h; (iv) 4-Cl-2,5-dimethoxyaniline, isopropanol, reflux, 3 h; (v) Fe, HOAc, NaOAc, CH_3OH, reflux, 3 h; (vi) 4-dimethylaminocrotonic acid hydrochloride, $(COCl)_2$, CH_3CN, NMP, 55 °C, 20 min; (vii) CAN, CH_3CN, H_2O; (viii) ROH, $CHCl_3$ or CH_2Cl_2, Et_3N or NaOPh 25–40 °C, 3–5 h.

A number of other reference compounds were used in this study and are shown in Schemes 1 and 3. Compounds **1** and **2** were optimized to be irreversible inhibitors of EGFR/Her2 kinases. The quinazoline **28** is a known ATP-competitive EGFR inhibitor.[33] Compound **29** (Gefitinib)[34] is a marketed ATP-competitive EGFR inhibitor. The phthalazine derivative **30** is reported to be a selective, reversibly binding, VEGFR-2 inhibitor.[35] The quinazoline **31** (ZD6474)[36] is a reversible binding VEGFR-2 inhibitor that is known to also have EGFR inhibitory properties. Compounds **32**–**34** are from our earlier work[19] and are irreversible VEGFR-2 kinase inhibitors.

3. Molecular modeling

A binding model for inhibitor **19** at the active site in EGFR is presented in Figure 1. The initial protein coordinates used in this study are those reported in the X-ray crystal structure of the complex between Erlotinib and the catalytic domain of EGFR.[37] The ligand was removed from this crystal structure and, with the exception of the water molecule that bridges the N3 atom of the quinazoline and Thr-766, the water molecules were removed. The inhibitor was docked using the GLIDE[38] docking algorithm in the XP (extra precision) mode. The resulting model shows the inhibitor oriented in a manner consistent with the way other quinazoline derivatives have been shown to bind to different kinases.[37,39]

In the most favored bound conformation, the oxygen atom of a quinone carbonyl group makes an intramolecular H-bond to the NH substituent on the quinazoline. This is similar to the low energy conformations found for the similar unbound inhibitors based on molecular mechanics calculations. A favorable interaction between the quinazoline N1 of **19** and the hinge region backbone NH of Met-769 is found to be significant in our model.

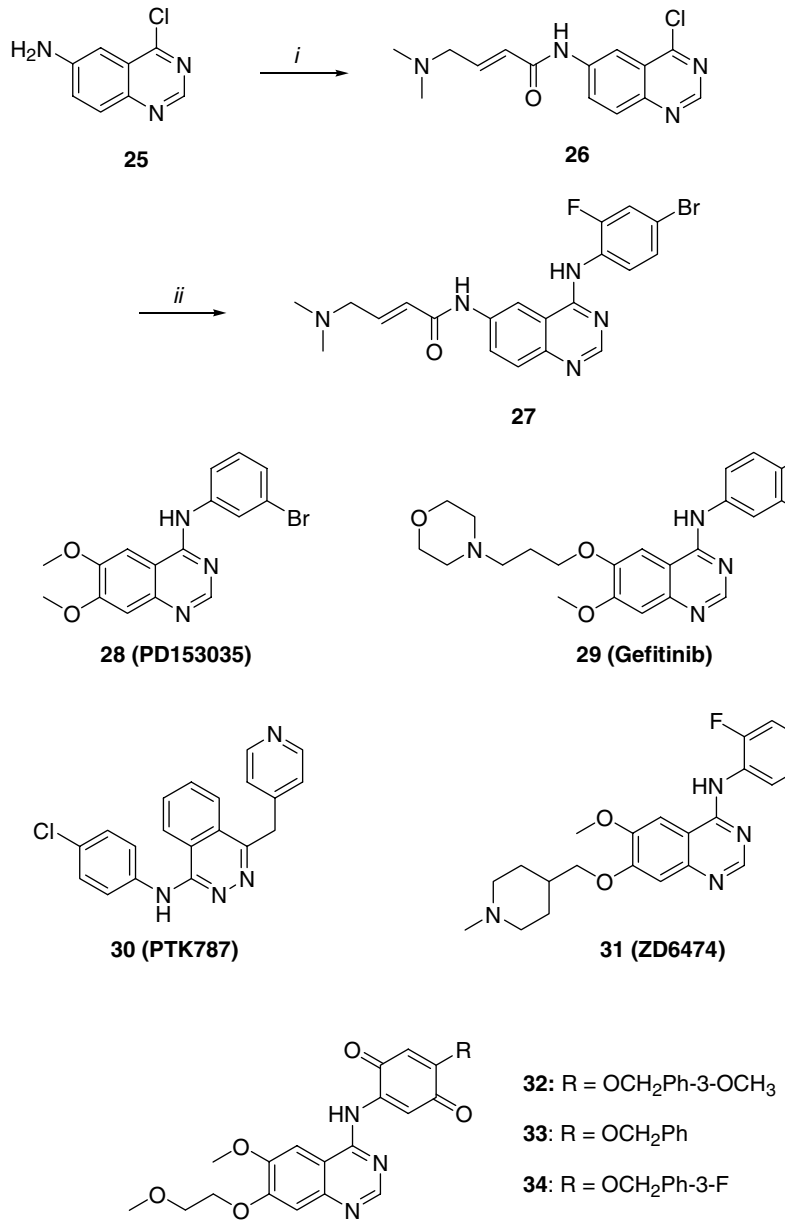

Scheme 3. Reagents and conditions: (i) 4-dimethylaminocrotonic acid hydrochloride, CH_3CN, NMP, $(COCl)_2$, 55 °C, 30 min; (ii) NMP, 4-Br-2-F-aniline, Py·HCl, isopropanol, 85 °C, 30 min.

The polar aromatic hydrogen atom on C2 of the quinazoline ring is favorably oriented at approximately 2.4 Å from the backbone carbonyl of Gln-767. The N3 atom of the quinazoline is H-bonded to the hydroxyl group of Thr-766 via a water bridge. A favorable face-to-face π–stacking interaction is evident between the benzyloxy quinone substituent and the aromatic ring of Phe-832. Finally, the sulfhydryl group of Cys-773 is located 6.0 Å away from the β-carbon atom of the Michael acceptor. A 10-picosecond molecular dynamics simulation of the protein–ligand complex revealed that this distance approached to within 3.0 Å, suggesting the feasibility of covalent bond formation (see Fig. 2).

A binding model for inhibitor **19** at the active site in VEGFR-2 is presented in Figure 3. The initial protein coordinates used in this study are those reported in the X-ray crystal structure of the catalytic domain of the enzyme.[40] The inhibitor was docked into the active site as described above. The bound conformation of **19** in VEGFR-2 is very similar to that found in EGFR (see Fig. 4) as are the specific interactions it makes with the protein. In this case, N1 of the quinazoline makes a hinge region interaction with the NH of Cys-919. The polar aromatic hydrogen atom on C2 of the quinazoline ring is favorably oriented at approximately 2.2 Å from the backbone carbonyl of Glu-917. As with the EGFR complex, we observe a favorable interaction between the benzyloxy quinone substituent of **19** and the aromatic ring of Phe-1047; however, in this case, the aromatic rings are oriented in an edge-to-face manner. Significantly, the center of the quinone ring is

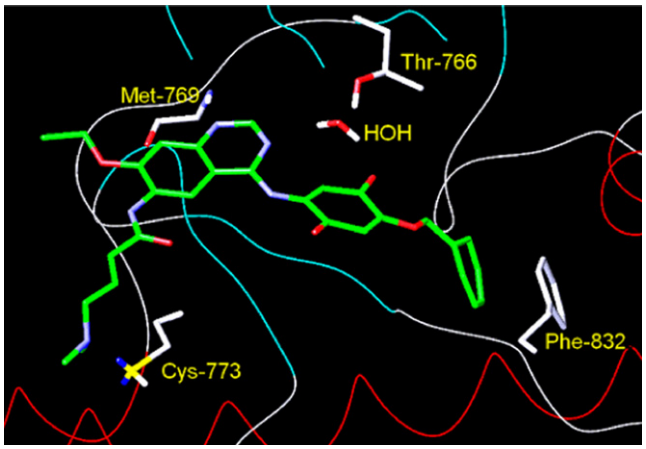

Figure 1. Proposed binding model for **19** bound to the kinase domain of EGFR.

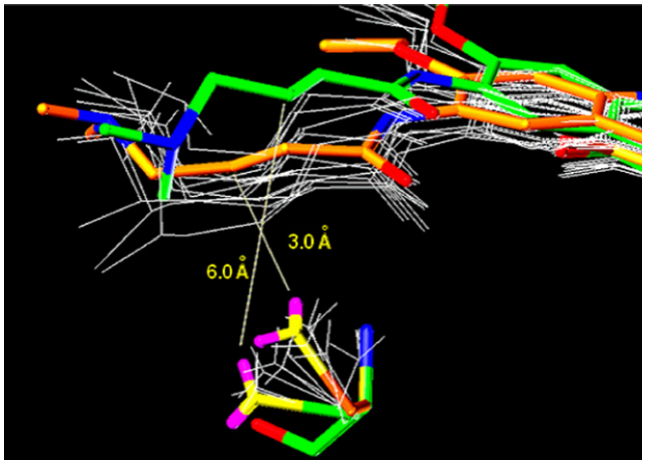

Figure 2. A view of the dynamics simulation for **19** bound to EGFR kinase in the region of the Michael acceptor showing the initial structure (green), intermediate structures (white), and final structure (orange). Note that a lone pair on the sulfhydryl group of Cys-733 approached the β-carbon atom of the Michael acceptor to within 3.0 Å during this dynamics run.

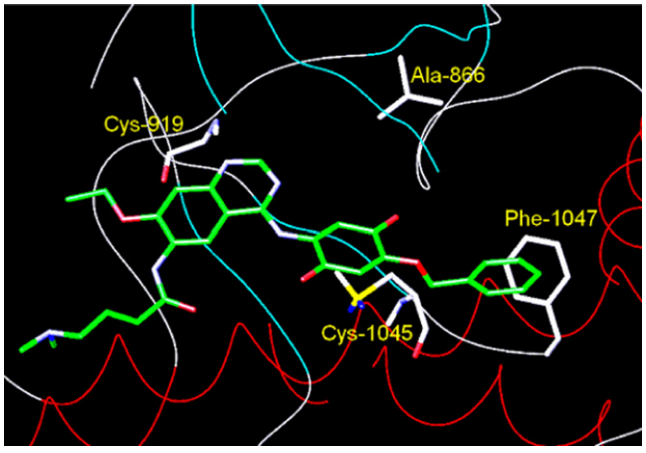

Figure 3. Proposed binding model for **19** bound to the kinase domain of VEGFR-2.

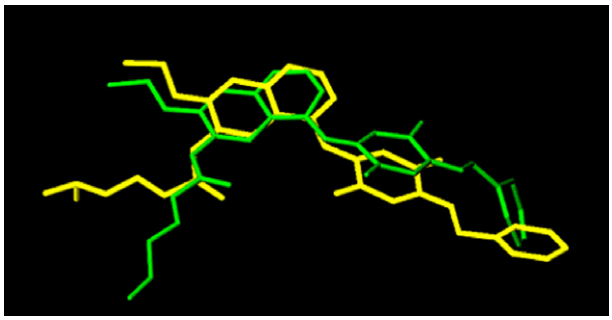

Figure 4. Overlap of **19** bound to EGFR (green) and VEGFR-2 (yellow) using the coordinated system defined by the overlapped proteins.

perpendicularly oriented toward the sulfhydryl group of Cys-1045, being located about 4.2 Å away. A 10-picosecond molecular dynamics simulation of the protein–ligand complex revealed that the lone pair on the sulfhydryl group of Cys-1045 approached the center of the quinone ring to within 3.7 Å (see Fig. 5). Previous molecular orbital calculations on related quinone-based inhibitors showed that the orbital density of the LUMO is largely localized on the quinone ring. It is evident from these simulations that the orbital overlap between the LUMO of **19** and an orbital centered on the sulfhydryl group of Cys-1045 should be sufficient to initiate an electron transfer reaction resulting in a reductive addition of the sulfhydryl group to the quinone ring.

Interestingly, there is also a cysteine residue, Cys-751, located in the quinone binding region in the EGFR complex. In this case, however, the center of the quinone ring is located about 6.5 Å away from the sulfhydryl group of Cys-751 with the lone pairs of the sulfhydryl group pointing away from the quinone ring of the bound inhibitor. The distance changed minimally during the dynamics simulations. Therefore, because of a less favorable orientation for orbital overlap and a longer

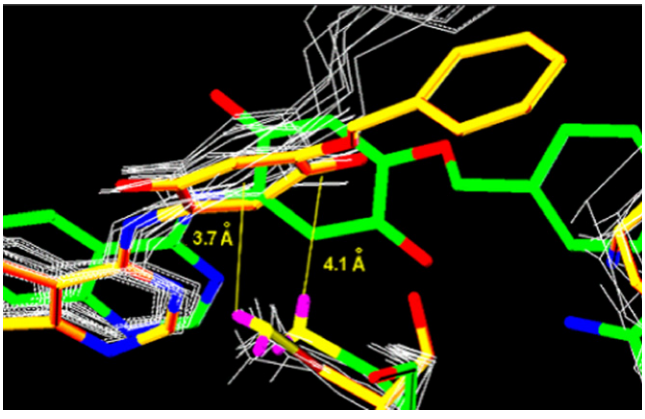

Figure 5. A view of the dynamics simulation for **19** bound to VEGFR-2 kinase in the region of the quinone ring showing the initial structure (green), intermediate structures (white), and final structure (orange). Note that a lone pair on the sulfhydryl group of Cys-1045 approached the center of the quinone ring to within approximately 3.7 Å during this dynamics run.

distance, one would not expect a covalent interaction to occur with this cysteine residue to a significant degree.

4. Results and discussion

The results of our biological assays are shown in Table 1. Our EGFR and VEGFR-2 assays are DELFIA® kinase assays[41] where a recombinant full cytoplasmic domain of human protein is utilized and where the activity of an inhibitor is expressed as an IC_{50}. For compounds where an IC_{50} could not be determined, the average % inhibition observed at the highest/lowest concentration tested is given. In order to assess the dependence of the IC_{50} values on the ATP concentration used in the assays, the EGFR and VEGFR-2 kinase assays were conducted using 1 μM and 1 mM concentrations of ATP. While the IC_{50} of a reversibly binding ATP-competitive inhibitor is a direct measure of the compound's ability to fit at the enzyme active site, the situation is expected to be more complicated for an irreversibly binding inhibitor where the IC_{50} will be a measure of both the fit at the active site, as well as the reactivity of the molecule. In this situation, one expects that for two molecules that fit the site equally well, the more reactive molecule will have a lower IC_{50} value. The IC_{50} value that we measure for a covalent binding inhibitor will be time dependent and additionally, depending on the rate of reaction of the inhibitor with the target enzyme, the IC_{50} value could simultaneously consist of components reflecting both reversible and irreversible binding.

Reference compounds, **1** and **2**, are known irreversible inhibitors of EGFR and their potent inhibitory activities in this respect were confirmed in this study. Neither compound was a potent inhibitor of VEGFR-2. Compound **29** (Gefitinib)[34] is a known ATP-competitive EGFR inhibitor and its activity in this respect was also confirmed in this study. It did not inhibit VEGFR-2 kinase significantly in our assay. Both the phthalazine **30**[35] and the quinazoline **31**[36] are reported to be ATP-competitive inhibitors of VEGFR-2 and we confirmed their activities against this target. They also showed modest EGFR kinase inhibitory activity.

It is clear from the data presented in Table 1 that each compound which has a quinone ring is an inhibitor of VEGFR-2 and each compound which has the 4-(dimethylamino)crotonamide Michael acceptor group is an inhibitor of EGFR. Compounds that have both types of reactive groups, **15**–**24**, inhibit both enzymes, many with good potency. It is instructive to compare compounds having a quinone ring but no Michael acceptor group, **32**–**34**, with the respective compounds having the same quinone substituents and also having the Michael acceptor group, **17**, **19**, and **23**. While the former compounds are potent VEGFR-2 inhibitors with IC_{50} values in the range 46.1–53.7 nM at 1 μM ATP, they lack the ability to inhibit EGFR significantly. In contrast, **17**, **19**, and **23** are relatively potent inhibitors of both enzymes. Similarly, the compounds that have a Michael acceptor but do not have the quinone ring, **1**, **2**, and **27**, are each potent inhibitors of EGFR, but

Table 1. Inhibition of EGFR and VEGFR-2 kinases[a]

Compound	EGFR					VEGFR-2				
	IC_{50} (nM) 1 μM ATP[b]	Avg % inh[c]	IC_{50} (nM) 1 mM ATP[d]	Avg % inh[c]	Ratio Hi/Lo ATP[e]	IC_{50} (nM) 1 μM ATP[f]	Avg % inh[c]	IC_{50} (nM) 1 mM ATP[g]	Avg % inh[c]	Ratio Hi/Lo ATP[e]
1	0.6		34.9		59.2	3131		>10,000	0	>3.2
2	0.08		0.18		2.3	858.2		>10,000	−4	>11.7
15	799.3		>10,000	24	>12.5	378.7		1397		3.7
16	283.3		2089		7.4	109.3		303.3		2.8
17	4.1		43.1		10.6	113.4		347.6		3.1
18	166.7		894.3		5.4	111.6		550.2		4.9
19	18.7		216.2		11.5	102.3		783.1		7.7
20	90.8		791.9		8.7	135.0		1009		7.5
21	12.2		35.6		2.9	80.2		178.8		2.2
22	47.5		295.2		6.2	76.2		298.0		3.9
23	107.3		346.9		3.2	371.5		1285		3.5
24	24.9		173.1		7.0	188.7		612.7		3.2
27	<10.0	64	704.0		>70.4	4389		>10,000	12	>2.3
28	2.6		>100	5	>38.7	1489		>10,000	17	>6.7
29	5.4		2753		505.3	>10,000	12	>10,000	6	>1.0
30	457.7		>10,000	46	>21.8	198.3		6754		34.1
31	112.4		>10,000	18	>89.0	27.3		4834		177.1
32	7710		>10,000	−13	>1.3	50.2		250		5.0
33	>10,000	20	>10,000	−30	>1.0	53.7		140		2.6
34	>10,000	34	>10,000	−27	>1.0	46.1		188		4.1

[a] The assays were conducted using the indicated ATP concentration. The IC_{50} is the concentration in nM needed to inhibit the phosphorylation of the protein substrate by 50% as determined from the dose–response curve. The IC_{50} values are averages of multiple determinations.
[b] The standard errors, on average, were 15% of the IC_{50} value.
[c] The % inhibition at the concentration shown in the left column.
[d] The standard errors, on average, were 18% of the IC_{50} value.
[e] The ratio of the IC_{50} values determined at 1 mM and 1 μM concentrations of ATP.
[f] The standard errors, on average, were 15% of the IC_{50} value.
[g] The standard errors, on average, were 17% of the IC_{50} value.

are very weak inhibitors of VEGFR-2. It is clear that the presence of the 4-(dimethylamino)crotonamide Michael acceptor group has altered the inhibitory profiles of these compounds resulting in improved EGFR activity, and that the presence of the quinone ring confers VEGFR-2 inhibitory activity.

With respect to the SAR within the group of proposed dual irreversible inhibitors **15**–**24**, **15** clearly stands out as being one of the least potent inhibitors of VEGFR-2. This is consistent with the results of our earlier study where we found that the 4-methoxy substituted quinone derivatives were among the less potent inhibitors.[19] We attributed this observation to the lower reactivity of such compounds as determined by the calculated LUMO energies and kinetic studies. It also appears that **15** is not a good inhibitor of EGFR despite the fact that it contains a 4-(dimethylamino)crotonamide Michael acceptor group. In this case, it is unlikely that the inherent reactivity of the Michael acceptor is significantly different in **15** compared to the other compounds in the series. One possible explanation for the inferior EGFR inhibitory activity in this case is that this compound has a lower initial binding affinity for the EGFR active site, which could result in a decreased rate of covalent bond formation. To be sure, this compound will lack the favorable interaction with the Phe-832 that is expected to be present with the 4-benzyloxy-type substituted compounds **17**–**24**. In a related observation, the 1,3-difluoro-2-propoxy derivative **16**, which also lacks this interaction, is a less potent inhibitor than the other compounds in the series **17**–**24** which can make such an interaction. Overall, the remaining compounds that are proposed to function as dual irreversible inhibitors, **17**–**24**, are each relatively potent inhibitors of both enzymes. We also note that there is not much variability in the potencies of **17**–**24** in inhibiting EGFR and VEGF-2, but this is to be expected given that these compounds were purposely designed to have similar structural features that were optimized in our earlier work.[15–17,19]

In our earlier studies with the EGFR/Her2 inhibitors **1** and **2**, we demonstrated that these compounds set up a covalent interaction with the targeted proteins by using radio-labeled drug.[15,16] In our other studies of the quinone-based irreversible inhibitors of VEGFR-2, we demonstrated covalent binding using mass spectral studies of the drug–protein complex.[19] In the present investigation, our evidence for covalent interaction will rely on the dependence of inhibitory activities on the concentration of ATP used in the assays. For compounds that function as conventional reversible inhibitors, we will expect to see a very significant increase in the IC_{50} values when changing the ATP concentration from 1 μM to 1 mM, while for irreversible inhibitors, since they should be effectively non-ATP-competitive, the changes in IC_{50} values are expected to be notably less, provided that the inhibitors are given sufficient time to react with the target cysteine residue.

As expected, the known reversible EGFR inhibitor **28** lost essentially all of its EGFR kinase inhibitory activity when the ATP concentration was raised from 1 μM to 1 mM. Likewise, the other reversible EGFR inhibitor **29** (Gefitinib) lost over 500-fold activity on increasing the ATP concentration. In contrast, for the known irreversible EGFR/Her2 kinase inhibitors **1** and **2**, while we did see a 58-fold decrease in potency in the EGFR kinase assay for **1** after raising the ATP concentration, we observed only about a 1-fold decrease in the potency for **2**. For the compounds **16**–**24**, which we are proposing function as dual irreversible inhibitors, we observed that the IC_{50} values increased on average only about 6-fold when the ATP concentration was raised from 1 μM to 1 mM. For several, the increase was only about 2- to 3-fold. The modest increase in the IC_{50} values we observe is consistent with these compounds functioning as irreversibly binding inhibitors of EGFR kinase.

For the known reversible VEGFR-2 inhibitors **30** and **31**, VEGFR-2 kinase inhibitory activity decreased significantly with increasing the ATP concentration from 1 μM to 1 mM with a 33- and 176-fold increase in IC_{50} values observed for these compounds, respectively. The compound **27** that has a Michael acceptor and headpiece designed to confer reversible binding VEGFR-2 activity was not very potent in our VEGFR-2 assays to begin with and it is therefore difficult to assess the effects on potency of increasing the ATP concentration for this analog. For those compounds that have a quinone ring and no Michael acceptor, **32**–**34**, as expected for irreversible inhibitors of VEGFR-2, we observed a less significant increase (3- to 4-fold) in the IC_{50} values on raising the ATP concentration. Most significantly, for the compounds that are proposed to function as dual irreversible inhibitors of both EGFR and VEGFR-2 kinases, **15**–**24**, we observed a minimal increase in the VEGFR-2 IC_{50} values on changing the ATP concentration from 1 μM to 1 mM. On average, the increase was only about 3-fold with the range being 2- to 8-fold. The modest increase in the IC_{50} values we see is consistent with these compounds functioning as irreversibly binding inhibitors of VEGFR-2 kinase.

In earlier studies[15–17] we showed, by unambiguous means, that quinazoline and 3-cyanoquinoline-based inhibitors having a 6-(4-(dimethylamino)crotonamide) Michael acceptor group are capable of functioning as irreversible EGFR/Her2 inhibitors. We also showed, again unambiguously, that quinazoline-based inhibitors having a 4-(amino-[1,4]benzoquinone) moiety can function as irreversible inhibitors of VEGR-2.[19] These earlier studies, combined with the in vitro studies presented herein, are consistent with our hypothesis that it would be possible to construct compounds such as **15**–**24** that function as dual irreversible inhibitors of both EGFR and VEGFR-2 kinases by targeting different, non-conserved, cysteine residues in each protein using molecules having two separate reactive centers. The purpose of the present study was simply to explore this hypothesis. Clearly, further evaluations such as selectivity studies and testing in cell-based assays and xenograft models will be needed to determine if this concept has any practical utility for the treatment of cancer.

5. Experimental section

5.1. Molecular modeling

The inhibitor structures were minimized using the MMFF94 force field in Sybyl.[42] A public domain crystal structure of EGFR[37] and that of VEGFR-2[40] were used as the 3-D representations for molecular docking studies. The inhibitor structures were docked using the GLIDE[38] docking algorithm in the XP (extra precision) mode. Details of the algorithm are found in GLIDE documentation. Briefly, GLIDEs proprietary conformational expansion and exhaustive search of the binding site produces a multitude of ligand poses which undergo an initial refinement, energy minimization on a pre-computed grid, and a final scoring and ranking. GLIDE uses proprietary scoring functions that are variations of the ChemScore[43] empirical scoring function and the OPLS-AA[44] force field to compute van der Waals and electrostatic grids for the receptor. The final ligand binding poses are ranked according to a computed Emodel score that encompasses the grid score, the proprietary Glide Score, and the internal energy strain. The low-energy protein–ligand complexes from these docking studies were used as starting points for molecular dynamics simulation studies using the MMFF94 force field in Sybyl.[42] Frames from trajectories of 10 picosecond (ps) simulations carried out at 300 °K at a stepsize of 10 femtoseconds (fs) were selected to represent the molecular motion of the protein–ligand complexes (see Figs. 2 and 5). In an effort to conserve computational resources, only the ligand and residues within an 8 Å radius were allowed to move. The remainder of the protein was formed into an aggregate. The function of the aggregate is to accommodate the movement of the selected region. As the binding site water molecule of the EGFR crystal structure was retained in these computational studies, the water molecule was included in the aggregate during the molecular dynamics simulation.

5.2. Biology

VEGFR-2 and EGFR kinase assays. The cytoplasmic domain (Val 805–Val 1356) of human VEGFR-2 was expressed in Sf9 cells and purified to >90% by sequential chromatography. EGFR kinase was purchased from Sigma (E3641). Kinase activity was evaluated using a DELFIA® (dissociation-enhanced lanthanide fluorescent immunoassay).[41] Assay conditions (enzyme, peptide, ATP, and time) were adjusted for each kinase such that reactions proceeded under linear kinetics. Nunc Maxisorb 96-well plates were coated for 1 h with poly(Glu_4-Tyr) peptide (Sigma) at a final concentration of either 0.5 μg/mL (for VEGFR-2 assay) or 25 μg/mL (for EGFR assay) in Tris-buffered saline (TBS) (25 mM Tris, pH 7.2, 150 mM NaCl) and then washed two times with TBS. VEGFR-2 or EGFR enzyme was diluted into kinase reaction buffer and incubated with compounds (prepared in 100% dimethylsulfoxide (DMSO)) for 10 min (for VEGFR-2) or 20 min (for EGFR). ATP/$MgCl_2$ was added to each well to initiate the reaction. Final concentrations of the assay components were: 1 μM ATP, 10 mM $MgCl_2$, 1 mM $MnCl_2$, 4 mM HEPES, pH 7.4, 20 μM Na_3VO_4, 20 μg/mL BSA, and 2% DMSO. After 40 min at room temperature, liquid was removed and plates were washed three times with TBST (TBS with 0.05% Tween 20). The wells were then incubated for 1 h at room temperature with 75 μl of ~0.1 μg/mL europium-conjugated anti-phosphotyrosine antibody (PT66; Perkin Elmer Life Sciences, Boston, MA) prepared in Assay Buffer (Perkin Elmer). Plates were washed three times with TBST and then incubated for 15 min in the dark with 100 μl of Enhancement Solution (Perkin Elmer). Plates were read in a Victor-V multi-label counter (Perkin Elmer) using the default europium detection protocol. Percent inhibition or IC_{50} of compounds were calculated by comparison with DMSO-treated control wells using model 201 of XLfit version 4.2 (IDBS).

In addition to the assay described above, assays were also conducted in a similar manner in the presence of 1000 μM ATP in order to determine the dependence of the IC_{50} values on the ATP concentration.

5.3. Chemistry

^1H NMR spectra were determined with a Bruker DRX400 spectrometer at 400 MHz. Chemical shifts, δ, are in parts per million relative to the internal standard tetramethylsilane. Electrospray (ES) mass spectra were recorded in positive mode on a Micromass Platform spectrometer. Some high-resolution electrospray mass spectra with higher precision were obtained on a Bruker 9.4T FTMS spectrometer. Chromatographic purifications were performed by flash chromatography using Baker 40μ silica gel. Analytical HPLC was conducted on an HP 1090 liquid chromatography system over a 4.6 × 150 mm YMC ODS-A column (5 μm, 120 Å) using multiple wavelength UV detection (typically 230 and 254 nm) unless stated otherwise.

5.4. 7-Ethoxy-6-nitroquinazolin-4-ol (9)

To the solution of Na (10.88 g, 473.37 mmol) in 660 mL EtOH was added 33 g (157.79 mmol) of 7-fluoro-6-nitro-3*H*-quinazolin-4-one, **8**.[29] The reaction mixture was stirred at reflux for 1.5 h. It was then poured into dilute NH_4Cl. The solid was collected and washed with H_2O. The solid was boiled in 1200 mL EtOH and cooled over the weekend. The resulting solid was collected and washed with ether to give 31.7 g (85%) of **9** as a light tan solid: MS (ESI) *m*/*z* 236.1 $(M+H)^{+1}$; ^1H NMR (400 MHz, DMSO-d_6) δ 1.39 (t, J = 4 Hz, 3H), 4.34 (q, J = 6.97 Hz, 2H), 7.41 (s, 1H), 8.22 (s, 1H), 8.51 (s, 1H), 12.49 (s, 1H).

5.5. 4-Chloro-7-ethoxy-6-nitroquinazoline (10)

A mixture of **9** (31.7 g, 134.78 mmol), 235 mL $SOCl_2$, and three drops of DMF was stirred at reflux for 3.5 h. Excess $SOCl_2$ was removed on the rotoevaporator. The reaction was stirred in 600 mL $CHCl_3$ and then cooled to 0 °C. The mixture was washed with cold $NaHCO_3$ and then dried over $MgSO_4$. The solution was passed through a pad of magnesol and washed with $CHCl_3$ and EtOAc. The solvent of the filtrate was

removed to give 33.2 g (97%) of **10** as a white solid. The compound was used without further purification: MS (ESI) *m/z* 254.0 $(M+H)^{+1}$; ^1H NMR (400 MHz, $CDCL_3$) δ 1.56 (t, $J = 4$ Hz, 3H), 4.34 (q, $J = 8$ Hz, 2H), 7.52 (s, 1H), 8.61 (s, 1H), 9.04 (s, 1H).

5.6. *N*-(4-Chloro-2,5-dimethoxyphenyl)-7-ethoxy-6-nitroquinazolin-4-amine (11)

A mixture of **10** (24.2 g, 95.41 mmol) and 4-chloro-2,5-dimethoxyaniline (17.9 g, 95.41 mmol) in 1.3 L isopropanol was stirred at reflux for 3 h. The solution was allowed to stand at room temperature overnight. The solid was collected and washed with ether to give 37.3 g (89%) of **11** as an orange powder. The compound was used without further purification: MS (ESI) *m/z* 405.1 $(M+H)^{+1}$; ^1H NMR (400 MHz, DMSO-d_6) δ 1.44 (t, $J = 6.92$ Hz, 3H), 3.77 (s, 3H), 3.79 (s, 3H), 4.39 (q, $J = 6.97$ Hz, 2H), 7.21 (s, 1H), 7.33(s, 1H), 7.59 (s, 1H), 8.78 (s, 1H), 9.43 (s, 1H), 11.36 (bs, 1H).

5.7. N^4-(4-Chloro-2,5-dimethoxyphenyl)-7-ethoxyquinazoline-4,6-diamine (12)

A mixture of **11** (37 g, 83.85 mmol), iron (28.1 g, 503.09 mmol), acetic acid (30.21 g, 503.09 mmol), and sodium acetate (6.88 g, 83.85 mmol) in 1.4 L CH_3OH was mechanically stirred at reflux for 3 h. To this mixture was added 50 mL NH_4OH. The boiling mixture was filtered. The solid was washed with hot CH_3OH. The solvent was removed from filtrate. The resulting solid was extracted with boiling acetone 4× and filtered. The acetone extracts were concentrated. The residue was recrystallized from EtOAc to yield 28.7 g (91%) of **12** as light tan solid. The compound was used without further purification: MS (ESI) *m/z* 375.1 $(M+H)^{+1}$; ^1H NMR (400 MHz, DMSO-d_6) δ 1.44 (t, $J = 7.05$ Hz, 3H), 3.82 (s, 3H), 3.85 (s, 3H), 4.21 (q, $J = 6.97$ Hz, 2H), 5.41 (s, 2H), 7.07 (s, 1H), 7.18 (s, 1H), 7.20 (s, 1H), 8.12 (s, 1H), 8.33 (s, 1H), 8.41 (s, 1H).

5.8. (2*E*)-*N*-{4-[(4-Chloro-2,5-dimethoxyphenyl)amino]-7-ethoxyquinazolin-6-yl}-4-(dimethylamino)but-2-enamide (13)

The (*E*)-4-(dimethylamino)-2-butenoic acid hydrochloride salt (4.42 g, 26.68 mmol), oxalyl chloride (4.42 g, 26.68 mmol), and a trace of DMF in 57 mL CH_3CN were stirred at 55 °C for 20 min. About half of the solvent was removed at reduced pressure at 50 °C and the solution was cooled. A solution of **12** (5 g, 13.34 mmol) in warm NMP (57 mL) was added over 10 min. The reaction mixture was stirred at 0 °C for 2 h. and diluted with dilute aqueous $NaHCO_3$. The resulting solid was collected, dissolved in hot THF, diluted with EtOAc, dried over $MgSO_4$, and filtered. The filtrate was passed through a column of silica gel, eluting with EtOAc, EtOAc/MeOH, and 700:300:10 EtOAc/MeOH/Et_3N. The solvent was removed from product fractions. The resulting solid was stirred in ether and collected to yield 5 g (77%) of **13** as a white solid: MS (ESI) *m/z* 486.1 $(M+H)^{+1}$; MS (ESI) *m/z* 243.5 $(M+2H)^{+2}$; ^1H NMR (400 MHz, DMSO-d_6) δ 1.46 (t, $J = 4$ Hz, 3H), 2.21 (s, 6H), 3.12 (d, $J = 4$ Hz, 2H), 3.77 (s, 3H), 3.80 (s, 3H), 4.29 (dd, $J = 12$, 8 Hz, 2H), 6.60 (d, $J = 16$ Hz, 1H), 6.77–6.83 (m, 1H), 7.18–7.26 (m, 2H), 7.60 (s, 1H), 8.40 (s, 1H), 8.91 (s, 1H), 9.15 (s, 1H), 9.48 (s, 1H).

5.9. (2*E*)-4-(Dimethylamino)-*N*-{7-ethoxy-4-[(4-methoxy-3,6- dioxocyclohexa-1,4-dien-1-yl)amino]quinazolin-6-yl}but-2-enamide (15)

A sample of 1.57 g (3.23 mmol) of **13** was boiled in 80 mL CH_3CN to dissolve most of the solid. To this was added 36 mL H_2O and the mixture was cooled to room temperature. To the stirred mixture was added 4.25 g (7.75 mmol) of solid ceric ammonium nitrate. The reaction mixture was stirred at room temperature for 2.5 h. The mixture was diluted in 700 mL $CHCl_3$ and 50 mL of saturated aqueous $NaHCO_3$. The mixture was filtered through Celite. The solid-Celite mixture was washed several times with a total volume of 1400 mL $CHCl_3$. The organic layer was separated and washed with H_2O giving a $CHCl_3$ solution of **14**.

To this was added 300 mL CH_3OH. The solution was dried over $MgSO_4$, filtered, and 50 mL Et_3N was added. The reaction mixture was heated to reflux for 2.75 h. The solvent was removed under vacuum and the residue was dissolved in $CHCl_3$ and washed with saturated aqueous Na2CO_3. The organic layer was dried over $MgSO_4$ and filtered through a short column of magnesol, eluting with $CHCl_3$ and then $CHCl_3$/EtOAc/MeOH = 500:500:50. The solvent was removed from the filtrate. The resulting solid was triturated with EtOAc and collected to give 0.85 g (58%) of **15** as an orange crystalline solid: MS (ESI) *m/z* 452.2 $(M+H)^{+1}$; ^1H NMR (400 MHz, $CDCl_3$) δ 1.59 (t, $J = 6.92$ Hz, 3H), 2.34 (s, 6H), 3.19–3.21 (m, 2H), 3.91 (s, 3H), 4.32 (q, $J = 6.88$ Hz, 2H), 6.00 (s, 1H), 6.25 (d, $J = 15.11$ Hz, 1H), 7.04–7.15 (m, 1H), 7.30 (s, 1H), 8.07 (s, 1H), 8.14 (s, 1H), 8.81 (s, 1H), 8.98 (s, 1H), 9.30 (s, 1H); Anal. Calcd for $C_{23}H_{25}N_5O_5$–(1.5 H_2O): C, 57.73; H, 5.90; N, 14.64. Found: C, 57.73; H, 5.90; N, 14.64.

5.10. (2*E*)-4-(Dimethylamino)-*N*-[7-ethoxy-4-({4-[2-fluoro-1-(fluoromethyl)ethoxy]-3,6-dioxocyclohexa-1,4-dien-1-yl}amino)quinazolin-6-yl]but-2-enamide (16)

This compound was prepared from **13** (0.86 g, 1.77 mmol) using CAN (2.33 g, 4.25 mmol) as described below, and then treated with 13.6 g (141.57 mmol) of 1,3-difluoro-2-propanol and 27 mL Et_3N using the procedure described above for **17**. In this instance, the reaction mixture was refluxed for 4 h. and then worked up in the usual manner, except the product was eluted from magnesol using CH_2Cl_2/EtOAc = 1:1. The solvent of the filtrate was removed. The resulting solid was swirled in CH_3CN-ether and filtered to give 0.38 g (42%) of **16** as an orange solid: HRMS: Calcd for $C_{25}H_{27}F_2N_5O_5 + H$, 516.20530; found (ESI-FTMS, $(M+H)^{+1}$), 516.20519; ^1H NMR (400 MHz, $CDCl_3$) δ 1.58 (t, $J = 7.05$ Hz, 3H), 2.39 (s, 6H), 3.26 (d, $J = 4.53$ Hz, 2H), 4.32 (m, $J = 6.80$ Hz, 3H), 4.69-4.81 (m, 4H), 6.14 (s, 1H), 6.29 (d, $J = 15.11$ Hz, 1H),

7.04-7.15 (m, 1H), 7.28 (s, 1H), 8.08 (s, 1H), 8.17 (s, 1H), 8.81 (s, 1H), 8.89 (s, 1H), 9.27(s, 1H); Anal. Calcd for $C_{25}H_{27}F_2N_5O_5$–(0.8 H_2O): C, 56.65; H, 5.44; N, 13.22. Found: C, 56.91; H, 5.28; N, 13.51.

5.11. (2*E*)-4-(Dimethylamino)-*N*-[7-ethoxy-4-({4-[(3-fluorobenzyl)oxy]-3,6-dioxocyclohexa-1,4-dien-1-yl}amino)quinazolin-6-yl]but-2-enamide (17)

A 0.8 g (1.65 mmol) sample of **13** was boiled in 40 mL CH_3CN. To this solution was added 20 mL H_2O and it was allowed to cool to room temperature. To this was added 2.17 g (3.95 mmol) of solid ceric ammonium nitrate. The reaction mixture was stirred at room temperature for 1.75 h. and was then diluted with 700 mL $CHCl_3$ and 25 mL of saturated aqueous Na_2CO_3. The mixture was extracted 4× with a total of 900 mL $CHCl_3$. 3-Fluorobenzyl alcohol (8.31 g, 65.85 mmol) was added. The mixture was dried over $MgSO_4$, filtered, and 25 mL Et_3N was added. The reaction mixture was refluxed under N_2 for 3.5 h. The reaction mixture was washed with saturated $NaHCO_3$. The organic layer was dried over $MgSO_4$. The solvent was removed in vacuum. The residue was dissolved in CH_2Cl_2. It was then filtered through a short column of magnesol and eluted with $CHCl_3$, then $CHCl_3$/EtOAc/isopropanol = 250:250:75. The solvent of the filtrate was removed. The resulting solid was triturated with CH_3CN-ether and filtered to give 0.16 g (18%) of **17** as an orange powder: HRMS: Calcd for $C_{29}H_{28}FN_5O_5$ + H, 546.21472; found (ESI-FTMS, $(M+H)^{+1}$), 546.21347; ^1H NMR (400 MHz, $CDCl_3$) δ 1.59 (t, J = 6.92 Hz, 3H), 2.35 (s, 6H), 3.22 (d, J = 4.78 Hz, 2H), 4.32 (q, J = 6.80 Hz, 2H), 5.10 (s, 2H), 6.03 (s, 1H), 6.26 (d, J = 15.11 Hz, 1H), 7.03–7.13 (m, 2H), 7.16 (dd, J = 9.32, 2.27 Hz, 1H), 7.21 (d, J = 7.55 Hz, 1H), 7.30 (s, 1H), 7.35–7.42 (m, 1H), 8.08 (s, 1H), 8.15 (s, 1H), 8.81(s, 1H), 8.94 (s, 1H), 9.29 (s, 1H); Anal. Calcd for $C_{29}H_{28}FN_5O_5$–(0.7 H_2O): C, 62.39; H, 5.31; N, 12.55. Found: C, 62.61; H, 4.99; N, 12.90.

5.12. (2*E*)-*N*-[4-({4-[(3,4-Difluorobenzyl)oxy]-3,6-dioxocyclohexa-1,4-dien-1-yl}amino)-7-ethoxyquinazolin-6-yl]-4-(dimethylamino)but-2-enamide (18)

This compound was prepared from **13** (0.85 g, 1.75 mmol) which was oxidized with CAN (2.3 g, 4.2 mmol), extracted with $CHCl_3$, and then treated with 4.79 g (33.23 mmol) of 3,4-difluorobenzyl alcohol and 20 mL Et_3N using the procedure described above for **17**. In this instance, the solution was first concentrated to 500 mL $CHCl_3$ and the reaction mixture was refluxed for 3 h. It was then worked up and purified in the usual manner. The resulting solid was swirled in CH_3CN-ether and filtered to give 0.21 g (21%) of **18** as a dark red solid: MS (ESI) m/z 564.2 $(M+H)^{+1}$; ^1H NMR (400 MHz, $CDCl_3$) δ 1.59 (t, J = 6.92 Hz, 3H), 2.34 (s, 6H), 3.20 (d, J = 5.04 Hz, 2H), 4.32 (q, J = 6.80 Hz, 2H), 5.04 (s, 2H), 6.03 (s, 1H), 6.25 (d, J = 15.36 Hz, 1H), 7.05-7.13 (m, 1H), 7.16-7.23 (m, 2H), 7.28-7.33 (m, 2H), 8.08 (s, 1H), 8.15 (s, 1H), 8.82 (s, 1H), 8.93 (s, 1H), 9.29 (s, 1H); Anal. Calcd for $C_{29}H_{27}F_2N_5O_5$–(0.75 H_2O): C, 60.36; H, 4.98; N, 12.14. Found: C, 60.16; H, 4.56; N, 12.48.

5.13. (2*E*)-*N*-(4-{[4-(Benzyloxy)-3,6-dioxocyclohexa-1,4-dien-1-yl]amino}-7-ethoxyquinazolin-6-yl)-4-(dimethylamino)but-2-enamide (19)

A suspension of **13** (0.854 g, 1.76 mmol) and CAN (2.314 g, 4.22 mmol) in 40 mL CH_3CN and 20 mL H_2O was stirred at room temperature for 1 h. The reaction mixture was diluted with 50 mL CH_2Cl_2 and was treated with 50 mL of saturated aqueous Na_2CO_3. The resulting mixture was stirred for 30 min. It was then filtered through Celite and the Celite was washed with CH_2Cl_2. The filtrate was extracted (3×30 mL) with CH_2Cl_2. The organic layers were combined and dried over Na_2SO_4. To this was added 0.449 g (2.64 mmol) of NaOPh($3H_2O$), which was previously melted in benzyl alcohol (1.9 g, 17.6 mmol). The reaction mixture was concentrated on the rotary evaporator at 30–40 °C over 30 min. It was passed through a magnesol plug, which was eluted with CH_2Cl_2-isopropanol mixtures and finally with a CH_2Cl_2-isopropanol-Et_3N mixture. The solvent of the filtrate was concentrated to give 288 mg (31%) of **19** as a red solid: HRMS: Calcd for $C_{29}H_{29}N_5O_5$ + H, 528.22415; found (ESI-FTMS, $(M+H)^{+1}$), 528.22382; ^1H NMR (400 MHz, $CDCl_3$) δ 1.59 (t, J = 6.92 Hz, 3H), 2.32 (s, 6H), 3.18 (dd, J = 5.67, 1.38 Hz, 2H), 4.32 (q, J = 6.97 Hz, 2H), 5.12 (s, 2H), 6.06 (s, 1H), 6.15–6.34 (m, 1H), 7.05–7.14 (m, 1H), 7.30 (s, 1H), 7.33–7.48 (m, 5H), 8.07 (s, 1H), 8.14 (s, 1H), 8.81 (s, 1H), 8.95 (s, 1H), 9.29 (s, 1H); Anal. Calcd for $C_{29}H_{29}N_5O_5$–(0.5 H_2O): C, 64.91; H, 5.64; N, 13.05. Found: C, 64.60; H, 5.54; N, 13.05.

5.14. (2*E*)-4-(Dimethylamino)-*N*-(4-{[3,6-dioxo-4-(pyridin-2-ylmethoxy)cyclohexa-1,4-dien-1-yl]amino}-7-ethoxyquinazolin-6-yl)but-2-enamide (20)

This compound was prepared from **13** (1.084 g, 2.23 mmol), CAN (2.93 g, 5.35 mmol), NaOPh($3H_2O$) (0.379 g, 2.23 mmol), and pyridine-2-methanol (2.43 g, 22.3 mmol) using the procedure described above for **19**. The reaction mixture was worked up and purified in the usual manner to give 74 mg (6%) of **20** as a dark red solid: MS (ESI) m/z 529.1$(M+H)^{+1}$; MS (ESI) m/z 265 $(M+2H)^{+2}$; HRMS: Calcd for $C_{28}H_{28}N_6O_5$ + H, 529.21940; found (ESI-FTMS, $(M+H)^{+1}$), 529.21897; ^1H NMR (400 MHz, $CDCl_3$) δ 1.58 (t, J = 6.92 Hz, 3H), 2.44 (s, 6H), 3.32 (d, J = 5.29 Hz, 2H), 4.31 (q, J = 7.05 Hz, 2H), 5.24 (s, 2H), 6.13 (s, 1H), 6.33 (d, J = 15.11 Hz, 1H), 7.05–7.15 (m, 1H), 7.28–7.33 (m, 2H), 7.57 (d, J = 8.06 Hz, 1H), 7.73–7.81 (m, 1H), 8.07 (s, 1H), 8.20 (s, 1H), 8.62 (d, J = 4.28 Hz, 1H), 8.82 (s, 1H), 8.94 (s, 1H), 9.27 (s, 1H); Anal. Calcd for $C_{28}H_{28}N_6O_5$–(3 H_2O): C, 57.72; H, 5.88; N, 14.42. Found: C, 57.54; H, 5.13; N, 14.79.

5.15. (2*E*)-*N*-[4-({4-[(3-Chlorobenzyl)oxy]-3,6-dioxocyclohexa-1,4-dien-1-yl}amino)-7-ethoxyquinazolin-6-yl]-4-(dimethylamino)but-2-enamide (21)

To a stirred solution of **13** (0.829 g, 1.71 mmol) in 40 mL CH_3CN and 20 mL H_2O was added CAN (2.25 g, 4.1 mmol). After 1 h, 50 mL CH_2Cl_2 and 75 mL of saturated Na_2CO_3 were added. The reaction mixture was

stirred for 30 min. The suspension was passed through a pad of Celite and the pad was washed with CH_2Cl_2. The filtrate was extracted with CH_2Cl_2 (3×250 mL). The combined organic layers (about a total volume of 800 mL CH_2Cl_2) were dried over Na_2SO_4. To this was added 439 mg (2.57 mmol) of NaOPh($3H_2O$) that was previously melted in 3-chlorobenzyl alcohol (2 mL, 17.1 mmol). After stirring, the reaction mixture was concentrated and poured onto magnesol, which was eluted with CH_2Cl_2-isopropanol mixtures and finally with a CH_2Cl_2-isopropanol-Et_3N mixture. The solvent of the filtrate was removed to give 302 mg (31%) of **21** as an orange solid: MS (ESI) *m/z* 562.0 $(M+H)^{+1}$, 281.5 $(M+2H)^{+2}$; HRMS: Calcd for $C_{29}H_{28}ClN_5O_5$ + H, 562.18517; found (ESI-FTMS, $(M+H)^{+1}$), 562.18608; ^1H NMR (400 MHz, $CDCl_3$) δ 1.59 (s, 3H), 2.35 (s, 6H), 3.21 (dd, J = 5.79, 1.26 Hz, 2H), 4.33 (q, J = 6.97 Hz, 2H), 5.08 (s, 2H), 6.04 (s, 1H), 6.21–6.31 (m, 1H), 7.05–7.16 (m, 1H), 7.28–7.40 (m, 4H), 7.44 (s, 1H), 8.08 (s, 1H), 8.16 (s, 1H), 8.82 (s, 1H), 8.95 (s, 1H), 9.30 (s, 1H); Anal. Calcd for $C_{29}H_{28}ClN_5O_5$–(1.7 H_2O): C, 58.80; H, 5.35; N, 11.83. Found: C, 58.71; H, 5.08; N, 11.94.

5.16. (2*E*)-4-(Dimethylamino)-*N*-(4-{[3,6-dioxo-4-(2-thienylmethoxy)cyclohexa-1,4-dien-1-yl]amino}-7-ethoxyquinazolin-6-yl)but-2-enamide (22)

This was prepared from **13** (0.804 g, 1.64 mmol), CAN (2.72 g, 4.96 mmol), NaOPh($3H_2O$) (731.6 mg, 4.3 mmol), and 2-thiophenemethanol (3.12 mL, 33.09 mmol) as described above for **21** to give 86.3 mg (10%) of **22** as a red solid: MS (ESI) *m/z* 534.0 $(M+H)^{+1}$, 267.5 $(M+2H)^{+2}$; HRMS: Calcd for $C_{27}H_{27}N_5O_5S$ + H, 534.18057; found (ESI-FTMS, $[M+H]^{1+}$), 534.18094; ^1H NMR (400 MHz, $CDCl_3$) δ 1.59 (t, J = 7.05 Hz, 3H), 2.34 (s, 6H), 3.20 (dd, J = 5.67, 1.38 Hz, 2H), 4.32 (q, J = 6.97 Hz, 2H), 5.28 (s, 2H), 6.13 (s, 1H), 6.24 (d, J = 15.11 Hz, 1H), 6.95–7.16 (m, 2H), 7.20 (d, J = 2.77 Hz, 1H), 7.30 (s, 1H), 7.39 (dd, J = 5.04, 1.26 Hz, 1H), 8.07 (s, 1H), 8.15 (s, 1H), 8.81 (s, 1H), 8.96 (s, 1H), 9.30 (s, 1H); Anal. Calcd for $C_{27}H_{27}N_5O_5S$–(0.5 H_2O): C, 59.77; H, 5.20; N, 12.91. Found: C, 59.34; H, 4.91; N, 12.91.

5.17. (2*E*)-4-(Dimethylamino)-*N*-[7-ethoxy-4-({4-[(3-methoxybenzyl)oxy]-3,6-dioxocyclohexa-1,4-dien-1-yl}amino)-quinazolin-6-yl]but-2-enamide (23)

This was prepared from **13** (0.519 g, 1.06 mmol), CAN (1.404 g, 2.56 mmol), NaOPh ($3H_2O$) (167.38 mg, 0.985 mmol), and 3-methoxybenzyl alcohol (809 mL, 6.564 mmol) as described above for **21** to give 220 mg (37%) of **23** as a red solid: HRMS: Calcd for $C_{30}H_{31}N_5O_6$ + H, 558.23471; found (ESI-FTMS, $(M+H)^{+1}$), 558.23403; the purity of **23** was evaluated on two HPLC systems and found to be 100% (MeCN–H_2O, 40–90% gradient, retention time = 5.13 min) and 94.9% (MeOH–H_2O, 70–90% gradient, retention time = 13.01 min); ^1H NMR (400 MHz, $CDCl_3$) δ 1.58 (t, J = 7.05 Hz, 3H), 2.33 (s, 6H), 3.20 (d, J = 4.78 Hz, 2H), 3.83 (s, 3H), 4.31 (q, J = 6.88 Hz, 2H), 5.10 (s, 2H), 6.05 (s, 1H), 6.24 (d, J = 15.36 Hz, 1H), 6.90 (dd, J = 8.31, 2.01 Hz, 1H), 6.94–7.03 (m, 2H), 7.04–7.13 (m, 1H), 7.28–7.35 (m, 2H), 8.06 (s, 1H), 8.15 (s, 1H), 8.80 (s, 1H), 8.94 (s, 1H), 9.28 (s, 1H).

5.18. (2*E*)-4-(Dimethylamino)-*N*-[7-ethoxy-4-({4-[(3-methylbenzyl)oxy]-3,6-dioxocyclohexa-1,4-dien-1-yl}amino)quinazolin-6-yl]but-2-enamide (24)

This was prepared from **13** (0.854 g, 1.76 mmol), CAN (2.3 g, 4.2 mmol), NaOPh ($3H_2O$) (0.448 g, 2.69 mmol), and 3-methylbenzyl alcohol (2.15 g, 17.6 mmol) as described above for **21** to give 193 mg (20%) of **24** as a red solid: HRMS: Calcd for $C_{30}H_{31}N_5O_5$ + H, 542.23980; found (ESI-FTMS, $(M+H)^{+1}$), 542.23995; the purity of **24** was evaluated on two HPLC systems and found to be 98% (MeCN/H_2O 30–90, 230 nm) and 97% (MeOH/H_2O 70–90, 230 nm); ^1H NMR (400 MHz, $CDCl_3$) δ 1.58 (t, J = 7.05 Hz, 3H), 2.32 (s, 6H), 2.38 (s, 3H), 3.18 (dd, J = 5.54, 1.51 Hz, 2H), 4.31 (q, J = 7.05 Hz, 2H), 5.09 (s, 2H), 6.05 (s, 1H), 6.14–6.31 (m, 1H), 6.98–7.13 (m, 1H), 7.14–7.26 (m, 3H), 7.28–7.30 (m, 1H), 8.05 (s, 1H), 8.13 (s, 1H), 8.13 (s, 1H), 8.80 (s, 1H), 8.94 (s, 1H), 9.28 (s, 1H); Anal. Calcd for $C_{30}H_{31}N_5O_5$–(0.8 H_2O): C, 64.79; H, 5.91; N, 12.60. Found: C, 64.93; H, 5.54; N, 12.46.

5.19. 4-Dimethylamino-but-2-enoic acid(4-chloro-quinazolin-6-yl)-amide (26)

To a stirred suspension of 4-dimethylaminocrotonic acid hydrochloride (1.45 g, 4.4 mmol) in 17.5 mL CH_3CN at 25 °C was added 25 mL (0.25 mmol) of NMP followed by $(COCl)_2$ (0.76 mL, 8.8 mmol) in one portion. The reaction mixture was stirred at 55 °C for 30 min, evaporated to 1/3 volume, diluted with 7.5 mL NMP, and cooled to 0 °C. The resulting solution was treated with a slurry of **25**[32] (0.90 g, 5.0 mmol) and 10 mL NMP. The suspension was stirred at 25 °C for 30 min. The reaction mixture was stirred with 2.4 g (17.5 mmol) of K_2CO_3 in 80 mL H_2O and extracted with CH_2Cl_2 in three portions. The extract was washed with a small volume of dilute brine, dried over $MgSO_4$, and concentrated to give a solution of **26** (4.4 mmol) in NMP that was used as such in the subsequent step.

5.20. (2*E*)-*N*-{4-[(4-Bromo-2-fluorophenyl)amino]quinazolin-6-yl}-4- (dimethylamino)but-2-enamide (27)

A mixture of **26** (0.53 mmol in NMP solution, prepared as above), 4-bromo-2-fluoroaniline (114 mg, 0.6 mmol), pyridine hydrochloride (116 mg, 1.0 mmol), and 10 mL of isopropanol was stirred at 85 °C for 30 min, cooled, and concentrated. The residue was partitioned between aqueous K_2CO_3 (pH ~ 9) and EtOAc/MeOH = 20:1. The organic layer was washed with H_2O and brine, dried over $MgSO_4$, and concentrated. Chromatography of the residue on silica gel with CH_2Cl_2–EtOAc–MeOH–Et_3N gave 82 mg of the title compound as a tan solid: HRMS: Calcd for $C_{20}H_{19}BrFN_5O$ + H, 444.08298; found (ESI-FTMS, $(M+H)^{+1}$), 444.08479; ^1H NMR (DMSO-d_6): δ 2.29 (s, 6H), 3.20–3.26 (m, 2H), 6.39 (d, J = 15.36 Hz, 1H), 6.76–6.87 (m, 1H), 7.42–7.54 (m, 2H), 7.64 (dd, J = 9.95, 1.64 Hz, 1H), 7.77–7.81 (d, J = 12 Hz, 1H),

7.86 (dd, J = 8.81, 1.76 Hz, 1H), 8.41–8.45 (s, 1H), 8.83 (s, 1H), 9.86 (s, 1H), 10.47 (s, 1H); Anal. Calcd for $C_{20}H_{19}BrFN_5O$–(1.5 H_2O): C, 50.98; H, 4.83; N, 14.69. Found: C, 51.05; H, 4.72; N, 14.89.

Acknowledgments

The authors wish to thank Drs. Tarek Mansour, Lee Greenberger, and Janis Upeslacis for their support and encouragement. We also thank the members of the Wyeth Chemical Technologies group for analytical and spectral determinations.

References and notes

1. Denny, W. A. *Pharmacol. Ther.* **2002**, *93*, 253–261.
2. Bridges, A. J.; Denny, W. A.; Dobrusin, E. M.; Doherty, A. M.; Elliott, W. L.; Fry, D. W.; Hook, K.; Leopold, W. R.; McNamara, D. J.; Nelson, J. W.; Palmer, B. D.; Patmore, S.; Rewcastle, G. W.; Roberts, B. J.; Showalter, H. D. H.; Slintak, V.; Smaill, J. B.; Thompson, A. M.; Trumpp-Kallmeyer, S.; Vincent, P. W.; Winters, R. T.; Zhou, H. *R. Soc. Chem.* **2001**, *264*, 151–162.
3. Kwak, E. L.; Sordella, R.; Bell, D. W.; Godin-Heymann, N.; Okimoto, R. A.; Brannigan, B. W.; Harris, P. L.; Driscoll, D. R.; Fidias, P.; Lynch, T. J.; Rabindran, S. K.; McGinnis, J. P.; Wissner, A.; Sharma, S. V.; Isselbacher, K. J.; Settleman, J.; Haber, D. A. *Proc. Natl. Acad. Sci. U.S.A.* **2005**, *102*, 7665–7670.
4. Carter, T. A.; Wodicka, L. M.; Shah, N. P.; Velasco, A. M.; Fabian, M. A.; Treiber, D. K.; Milanov, Z. V.; Atteridge, C. E.; Biggs, W. H., Jr.; Edeen, P. T.; Floyd, M.; Ford, J. M.; Grotzfeld, R. M.; Herrgard, S.; Insko, D. E.; Mehta, S. A.; Patel, H. K.; Pao, W.; Sawyers, C. L.; Varmus, H.; Zarrinkar, P. P.; Lockhart, D. J. *Proc. Natl. Acad. Sci. U.S.A.* **2005**, *102*, 11011–11016.
5. Kobayashi, S.; Boggon, T. J.; Dayaram, T.; Jaenne, P. A.; Kocher, O.; Meyerson, M.; Johnson, B. E.; Eck, M. J.; Tenen, D. G.; Balizs, H. *N. Engl. J. Med.* **2005**, *352*, 786–792.
6. Kobayashi, S.; Ji, H.; Yuza, Y.; Meyerson, M.; Wong, K.-K.; Tenen, D. G.; Halmos, B. *Cancer Res.* **2005**, *65*, 7096–7101.
7. Greulich, H.; Chen, T. H.; Feng, W.; Janne, P. A.; Alvarez, J. V.; Zappaterra, M.; Bulme, r S. E.; Frank, D. A.; Hahn, W. C.; Sellers, W. R.; Meyerson, M. *PLoS Med.* **2005**, *2*, e313.
8. Yoshimura, N.; Kudoh, S.; Kimura, T.; Mitsuoka, S.; Matsuura, K.; Hirata, K.; Matsui, K.; Negoro, S.; Nakagawa, K.; Fukuoka, M. *Lung Cancer* **2006**, *51*, 363–368.
9. Cohen, M. S.; Zhang, C.; Shokat, K. M.; Taunton, J. *Science* **2005**, *308*, 1318–1321.
10. Shaul, M.; Abourbeh, G.; Jacobson, O.; Rozen, Y.; Laky, D.; Levitzki, A.; Mishani, E. *Bioorg. Med. Chem.* **2004**, *12*, 3421–3429.
11. Mishani, E.; Abourbeh, G.; Jacobson, O.; Dissoki, S.; Revital Ben, D.; Rozen, Y.; Shaul, M.; Levitzki, A. *J. Med. Chem.* **2005**, *48*, 5337–5348.
12. Andreas, S.; Jonathan, K.; Sumati, M.; Ralph, R.; Santi, D. V. *Proc. Natl. Acad. Sci. U.S.A.* **2006**, *103*, 4234–4239.
13. Tsou, H.-R.; Mamuya, N.; Johnson, B. D.; Reich, M. F.; Gruber, B. C.; Ye, F.; Nilakantan, R.; Shen, R.; Discafani, C.; DeBlanc, R.; Davis, R.; Koehn, F. E.; Greenberger, L. M.; Wang, Y.-F.; Wissner, A. *J. Med. Chem.* **2001**, 2719–2734.
14. Torrance, C. J.; Jackson, P. E.; Montgomery, E.; Kinzler, K. W.; Vogelstein, B.; Wissner, A.; Nunes, M.; Frost, P.; Discafani, C. M. *Nat. Med.* **2000**, *6*, 1024–1028.
15. Wissner, A.; Overbeek, E.; Reich, M. F.; Floyd, M. B.; Johnson, B. D.; Mamuya, N.; Rosfjord, E. C.; Discafani, C.; Davis, R.; Shi, X.; Rabindran, S. K.; Gruber, B. C.; Ye, F.; Hallett, W. A.; Nilakantan, R.; Shen, R.; Wang, Y.-F.; Greenberger, L. M.; Tsou, H.-R. *J. Med. Chem.* **2003**, *46*, 49–63.
16. Rabindran, S. K.; Discafani, C. M.; Rosfjord, E. C.; Baxter, M.; Floyd, M. B.; Golas, J.; Hallett, W. A.; Johnson, B. D.; Nilakantan, R.; Overbeek, E.; Reich, M. F.; Shen, R.; Shi, X.; Tsou, H.-R.; Wang, Y.-F.; Wissner, A. *Cancer Res.* **2004**, *64*, 3958–3965.
17. Tsou, H.-R.; Overbeek-Klumpers, E. G.; Hallett, W. A.; Reich, M. F.; Floyd, M. B.; Johnson, B. D.; Michalak, R. S.; Nilakantan, R.; Discafani, C.; Golas, J.; Rabindran, S. K.; Shen, R.; Shi, X.; Wang, Y.-F.; Upeslacis, J.; Wissner, A. *J. Med. Chem.* **2005**, *48*, 1107–1131.
18. Klutchko, S. R.; Zhou, H.; Winters, R. T.; Tran, T. P.; Bridges, A. J.; Althaus, I. W.; Amato, D. M.; Elliott, W. L.; Ellis, P. A.; Meade, M.; Roberts, B. J.; Fry, D. W.; Gonzales, A. J.; Harvey, P. J.; Nelson, J. M.; Sherwood, V.; Han, H.-K.; Pace, G.; Smaill, J. B.; Denny, W. A.; Hollis, S. H. D. *J. Med. Chem.* **2006**, *49*, 1475–1485.
19. Wissner, A.; Floyd, M. B.; Johnson, B. D.; Fraser, H.; Ingalls, C.; Nittoli, T.; Dushin, R. G.; Discafani, C.; Nilakantan, R.; Marini, J.; Ravi, M.; Cheung, K.; Tan, X.; Musto, S.; Annable, T.; Siegel, M. M.; Loganzo, F. *J. Med. Chem.* **2005**, *48*, 7560–7581.
20. Kari, C.; Chan, T. O.; Rocha de Quadros, M.; Rodeck, U. *Cancer Res.* **2003**, *63*, 1–5.
21. Salomon, D. S.; Brandt, R.; Ciardiello, F.; Normanno, N. *Crit. Rev. Oncol. Haematol.* **1995**, *19*, 183–232.
22. Gullick, W. J. *Br. Med. Bull.* **1991**, *47*, 87–98.
23. Woodburn, J. R. *Pharmacol. Ther.* **1999**, *82*, 241–250.
24. Carmeliet, P.; Jain, R. K. *Nature* **2000**, *407*, 249–257.
25. Folkman, J. *Semin. Oncol.* **2002**, *29*, 15–18.
26. Ferrara, N. *Oncologist* **2004**, *9*, 2–10.
27. Hicklin, D. J.; Ellis, L. M. *J. Clin. Oncol.* **2005**, *23*, 1011–1027.
28. Pandey, A.; Volkots, D. L.; Seroogy, J. M.; Rose, J. W.; Yu, J.-C.; Lambing, J. L.; Hutchaleelaha, A.; Hollenbach, S. J.; Abe, K.; Giese, N. A.; Scarborough, R. M. *J. Med. Chem.* **2002**, *45*, 3772–3793.
29. Rewcastle, G. W.; Palmer, B. D.; Bridges, A. J.; Showalter, H. D. H.; Sun, L.; Nelson, J.; McMichael, A.; Kraker, A. J.; Fry, D. W.; Denny, W. A. *J. Med. Chem.* **1996**, *39*, 918–928.
30. Wedge, S. R.; Kendrew, J.; Hennequin, L. F.; Valentine, P. J.; Barry, S. T.; Brave, S. R.; Smith, N. R.; James, N. H.; Dukes, M.; Curwen, J. O.; Chester, R.; Jackson, J. A.; Boffey, S. J.; Kilburn, L. L.; Barnett, S.; Richmond, G. H. P.; Wadsworth, P. F.; Walker, M.; Bigley, A. L.; Taylor, S. T.; Cooper, L.; Beck, S.; Juergensmeier, J. M.; Ogilvie, D. J. *Cancer Res.* **2005**, *65*, 4389–4400.
31. Rich, J. N.; Sathornsumetee, S.; Keir, S. T.; Kieran, M. W.; Laforme, A.; Kaipainen, A.; McLendon, R. E.; Graner, M. W.; Rasheed, B. K. A.; Wang, L.; Reardon, D. A.; Ryan, A. J.; Wheeler, C.; Dimery, I.; Bigner, D. D.; Friedman, H. S. *Clin. Cancer Res.* **2005**, *11*, 8145–8157.
32. Wissner, A.; Johnson, B. D.; Floyd, M. B., Jr.; Kitchen, D. B. U.S. PAT. 5760041, 1998.
33. Fry, D. W.; Kraker, A. J.; McMichael, A.; Ambroso, L. A.; Nelson, J. M.; Leopold, W. R.; Connors, R. W.; Bridges, A. J. *Science* **1994**, *265*, 1093–1095.
34. Wakeling, A. E.; Guy, S. P.; Woodburn, J. R.; Ashton, S. E.; Curry, B. J.; Barker, A. J.; Gibson, K. H. *Cancer Res.* **2002**, *62*, 5749–5754.

35. Bold, G.; Altmann, K.-H.; Frei, J.; Lang, M.; Manley, P. W.; Traxler, P.; Wietfeld, B.; Brueggen, J.; Buchdunger, E.; Cozens, R.; Ferrari, S.; Furet, P.; Hofmann, F.; Martiny-Baron, G.; Mestan, J.; Roesel, J.; Sills, M.; Stover, D.; Acemoglu, F.; Boss, E.; Emmenegger, R.; Lasser, L.; Masso, E.; Roth, R.; Schlachter, C.; Vetterli, W.; Wyss, D.; Wood, J. M. *J. Med. Chem.* **2000**, *43*, 2310–2323.
36. Hennequin, L. F.; Thomas, A. P.; Johnstone, C.; Stokes, E. S. E.; Plé, P. A.; Lohmann, J.-J. M.; Ogilvie, D. J.; Dukes, M.; Wedge, S. R.; Curwen, J. O.; Kendrew, J.; Lambert-van der Brempt, C. *J. Med. Chem.* **1999**, *42*, 5369–5389.
37. Stamos, J.; Sliwkowski, M. X.; Eigenbrot, C. *J. Biol. Chem.* **2002**, *277*, 46265–46272.
38. GLIDE; Schrodinger Software: Portland, OR, www.schrodinger.co.
39. Shewchuk, L.; Hassell, A.; Wisely, B.; Rocque, W.; Holmes, W.; Veal, J.; Kuyper, L. F. *J. Med. Chem.* **2000**, *43*, 133–138.
40. McTigue, M. A.; Wickersham, J. A.; Pinko, C.; Showalter, R. E.; Parast, C. V.; Tempczyk-Russell, A.; Gehring, M. R.; Mroczkowski, B.; Kan, C.-C.; Villafranca, J. E.; Appelt, K. *Struct. Fold. Des.* **1999**, *7*, 319–330.
41. Loganzo, F.; Hardy, C. A. *Am. Biotech. Lab.* **1998**, *16*, 26–28.
42. Sybyl 7.2; Tripos: St. Louis, MO.
43. Eldridge, M. D.; Murray, C. W.; Auton, T. R.; Paolini, G. V.; Mee, R. P. *J. Comput. Aided Mol. Des.* **1997**, *11*, 425–445.
44. Jorgensen, W. L.; Maxwell, D. S.; Tirado-Rives, J. *J. Am. Chem. Soc.* **1996**, *118*, 11225–11236.